Argonne NATIONAL LABORATORY

Conference Paper Manuscript

Comparisons of RELAP5-3D Analyses to Experimental Data from the Natural Convention Shutdown Heat Removal Test Facility

prepared by
Matthew Bucknor, Rui Hu, Darius Lisowski, and Adam Kraus

Nuclear Engineering Division
Argonne National Laboratory
9700 South Cass Avenue, Bldg. 208
Argonne, IL 60439-4854

2016 International Congress on Advances in Nuclear Power Plants
ICAPP 2016
April 17-20, 2016
San Francisco, CA
USA

Comparisons of RELAP5-3D Analyses to Experimental Data from the Natural Convention Shutdown Heat Removal Test Facility

Matthew Bucknor, Rui Hu, Darius Lisowski, Adam Kraus

Argonne National Laboratory, 9700 South Cass Ave., Argonne, IL 60439 USA
Email: mbucknor@anl.gov, rhu@anl.gov, dlisowski@anl.gov, arkraus@anl.gov

The Reactor Cavity Cooling System (RCCS) is an important passive safety system being incorporated into the overall safety strategy for high temperature advanced reactor concepts such as the High Temperature Gas-Cooled Reactors (HTGR). The Natural Convection Shutdown Heat Removal Test Facility (NSTF) at Argonne National Laboratory (Argonne) reflects a ½-scale model of the primary features of one conceptual air-cooled RCCS design. The project conducts ex-vessel, passive heat removal experiments in support of Department of Energy Office of Nuclear Energy's Advanced Reactor Technology (ART) program, while also generating data for code validation purposes. While experiments are being conducted at the NSTF to evaluate the feasibility of the passive RCCS, parallel modeling and simulation efforts are ongoing to support the design, fabrication, and operation of these natural convection systems. Both system-level and high fidelity computational fluid dynamics (CFD) analyses were performed to gain a complete understanding of the complex flow and heat transfer phenomena in natural convection systems. This paper provides a summary of the RELAP5-3D NSTF model development efforts and provides comparisons between simulation results and experimental data from the NSTF. Overall, the simulation results compared favorably to the experimental data, however, further analyses need to be conducted to investigate any identified differences.

I. INTRODUCTION

Advanced reactor designers continue to strive for increased resilience and reliability that will yield improvements in plant safety. This benefit is usually achieved through the utilization of passive systems, which require little to no electric power or human action for successful operation. One such system, the Reactor Cavity Cooling System (RCCS), is utilized in the General Atomics Modular High Temperature Gas-Cooled Reactor (GA-MHTGR) design[1].

I.A. Reactor Cavity Cooling System

The RCCS, shown in Fig. 1 (Ref. 1), uses natural convection to drive air from the environment through cold downcomers and into a lower plenum. The air then flows through hot riser tubes that surround the reactor guard vessel and line the inner wall of the concrete containment vessel. Heat from the guard vessel is transferred to the air in the hot riser tubes through a combination of radiation and convection and is ultimately rejected to the environment. The RCCS is designed to remove decay heat, but because it is completely passive (no baffle or damper operation is required), it also functions during normal reactor operation.

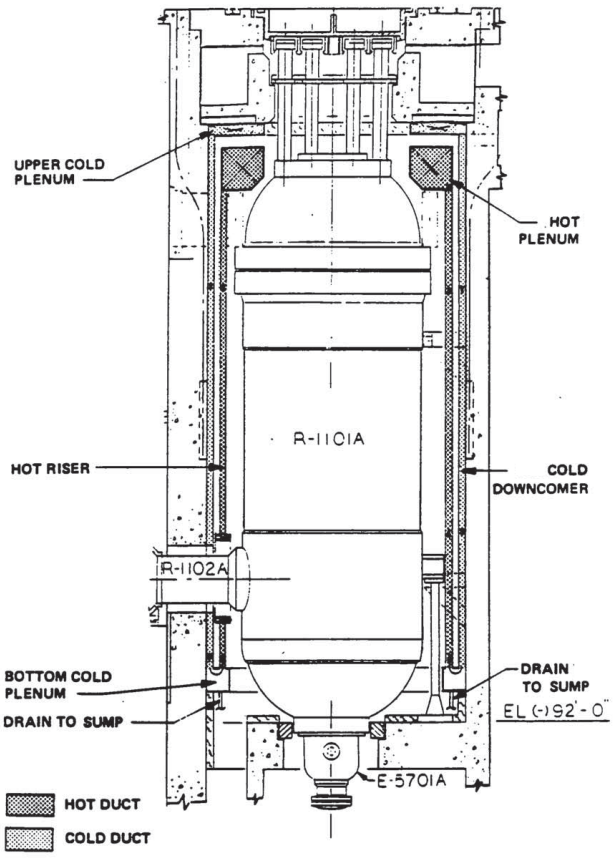

Fig. 1. GA-MHTGR RCCS (Ref. 1).

I.B. Natural Convection Shutdown Heat Removal Test Facility

The Natural convection Shutdown heat removal Test Facility (NSTF) (Ref. 2, 3, 4) is a large-scale thermal hydraulics test facility that has been built at Argonne National Laboratory (Argonne). The facility was constructed to carry out highly instrumented experiments to validate the performance of the RCCS while also generating data for code validation purposes.

The general facility layout is provided in Fig. 2 (Ref. 4). A heat flux is applied to the back cavity wall by an array of electric radiant heaters, which leads to the development of natural convection flow to cool the system. In a standard test, cold air is drawn from the building into the downcomer pipe and inlet plenum. Flow is then split between twelve riser ducts for the length of the heated cavity. These ducts all converge at an outlet plenum, where flow mixes and is then exhausted from the NSTF through two chimneys.

II. RELAP5-3D SYSTEM ANALYSIS OF NSTF

While CFD codes can be utilized to analyze steady-state behavior, transient analyses via CFD is computationally expensive and perhaps excessive if the goal of the analysis is to examine overall system behavior. System level codes such as RELAP5-3D (Ref. 5) provide the ability to analyze the response of a system during transients with minimal computational resources. For this reason, an existing RELAP5-3D model of the NSTF was updated to analyze the integrated system behavior. RELAP5-3D version 4.0.3 was utilized to perform the simulations described in this work.

A nodalization diagram of the current RELAP5-3D model of the NSTF is shown in Fig. 3. In the model, air enters the system from a time dependent volume (TD900 in Fig. 3) that represents the atmosphere inside Building 308 at Argonne where the facility is housed. Air flows through a downcomer (P910) and into the lower plenum (B920) before entering the hot riser ducts (P930). The air temperature increases as the air passes through the hot riser ducts and into the outlet plenum (B941). The air then flows from the outlet plenum into two chimney duct systems (represented as a single duct by P950-B960-B970-P980-P985) before being exhausted to a time dependent volume (TD990) that represent the atmosphere outside Building 308.

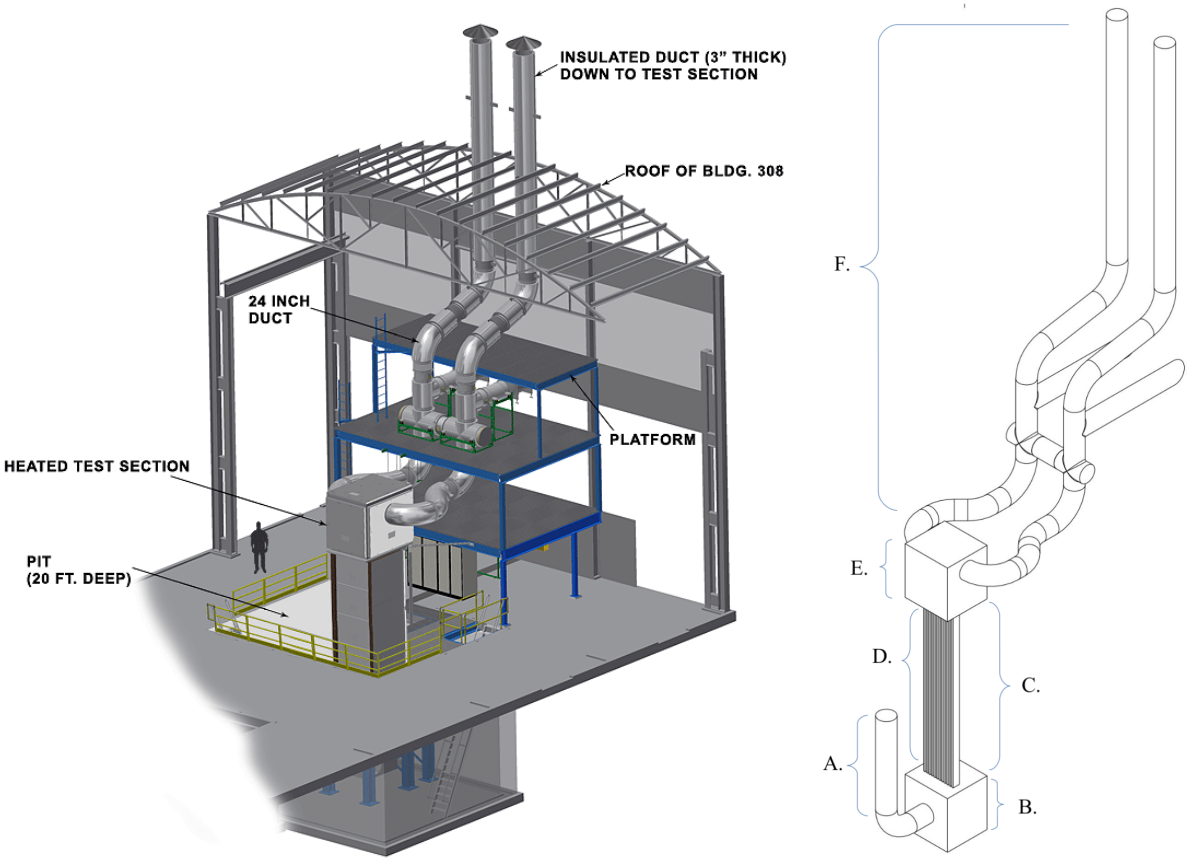

Fig. 2. NSTF Layout. Left: solid model rendering; Right: primary segments, A. inlet downcomer, B. inlet plenum, C. heated cavity, D. riser ducts, E. outlet plenum, F. chimney stacks[4].

The model also includes a fan loft pathway that is utilized during forced flow testing at the facility. During these forced flow tests, air is directed from B970 to TD975 and the flow path from B970 to P980 is blocked.

Heat structures are modeled on the upper plenum and on the main chimney ductwork in an attempt to treat the heat losses that occur from those components. These heat structures represent the metal walls of the components as well as any insulation material applied to the outside of the facility to reduce heat losses. Natural convection with ambient air is assumed at the outer surface of these heat structures.

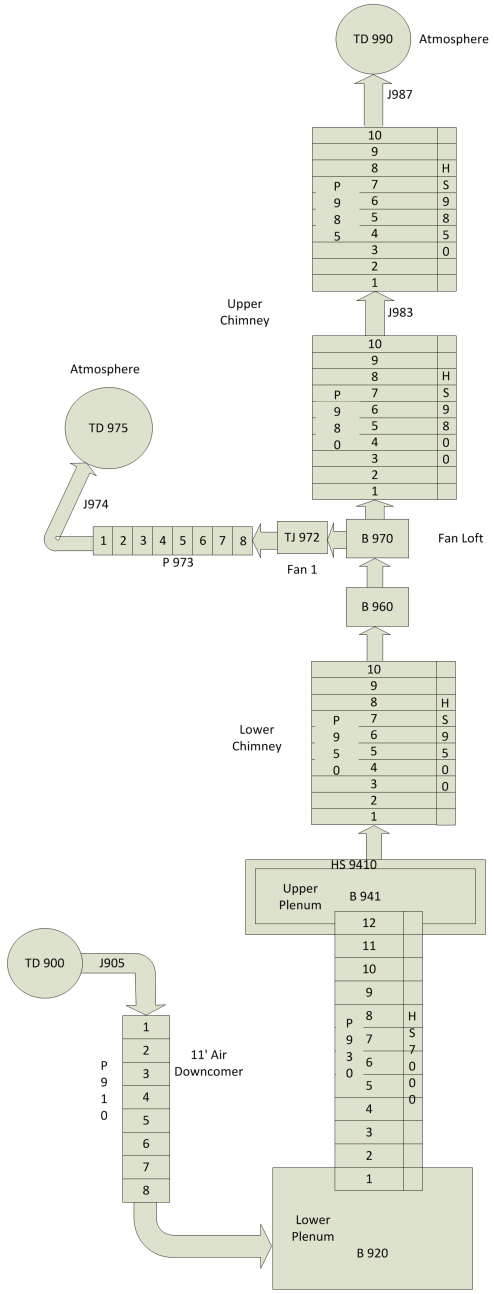

Fig. 3. RELAP5-3D nodalization diagram of the NSTF.

II.A. RELAP5-3D Model Development and Verification

Previous NSTF design analyses efforts at Argonne included the development of a RELAP5-3D model of the NSTF such that an existing model was available for use. However, preliminary analyses demonstrated that the simulation results of the model did not agree well with experimental data. Therefore, the previous model was utilized as a starting point for additional development.

The previous model was significantly modified to create a new (current) model of the NSTF. Not only were substantial geometry changes made to the previous model, many RELAP5-3D components were removed from the model in order to create a simplified model that could be more easily verified. Some modifications were made to eliminate numerical instabilities. The previous model included two separate (but identical) chimney stacks. This led to numerical flow instabilities during startup (low power, low flow conditions). To eliminate the instabilities, the two chimney stacks were combined into a single stack.

Changes were also made to account for the head loss associated with the Sierra flow conditioner located at the entrance to the downcomer. Given the short entrance length of the downcomer region, a flow conditioner is used to create a flat and known velocity profile. This eliminates the uncertainty associated with a developing parabolic profile and allows confidence in accurate flow measurements across the full span of anticipated regimes. Losses associated with the flow conditioner are relatively small, but not inconsequential to the performance of NSTF.

To account for the head loss associated with the flow condition, a form loss coefficient was added to the junction between the time-dependent volume that represents the atmosphere inside Building 308 and the downcomer. In RELAP5-3D, form loss coefficients can be modeled as a function of the Reynolds number using the following equation:

$$k = A + B * \mathrm{Re}^{-C} \qquad (1)$$

where, A, B, and C are user-defined constants and Re is the Reynolds number. Linear regression techniques and experimental data from the NSTF were utilized to determine appropriate values for A, B, and C. The resulting values for A, B, and C were input into RELAP5-3D and the *k*-loss values from RELAP5-3D were compared to the experimental data. The results of this comparison are shown in Fig. 4 and the resulting values for A, B, and C are provided in Table I along with validation results of the pressure drop across the flow conditioner.

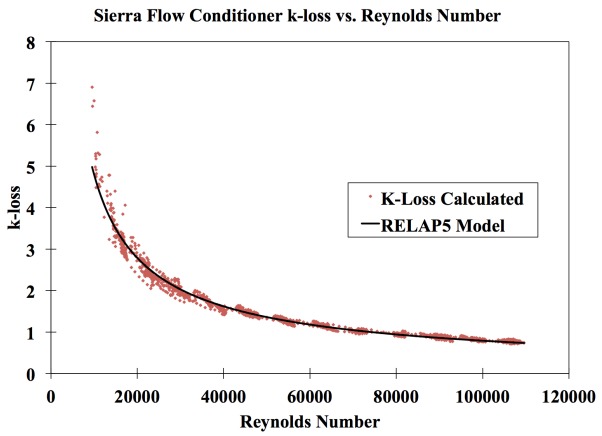

Fig. 4. *k*-losses associated with the Sierra Flow Conditioner.

TABLE I. Form Loss Equation Parameters and Model Validation Results for Pressure Drop Across the Sierra Flow Conditioner

Parameters	Values
A	0
B	6528.25
C	0.78
Mass Flow Rate	0.548 kg/s
Experimental Δp	1.72 Pa
RELAP5 Δp	1.73 Pa
Percent Error	0.58%

Hand calculations and comparisons to experimental results were performed to verify that the RELAP5-3D model was calculating the correct pressure drop across the hot riser ducts. A polynomial curve fit was applied to isothermal experimental data from the NSTF (see Fig. 5) to calculate the pressure drop at a mass flow rate of 0.548 kg/s. This mass flow rate was the steady-state mass flow rate of a previous natural circulation test performed at the NSTF. A forced flow (to ensure the mass flow rate was correct) RELAP5-3D simulation was performed with no heat addition and the resulting pressure drop was compared to the experimental data. The results of the comparison are provided in Table II. For turbulent flow (Reynolds number higher than 3000), the Zigrang-Sylvester approximation to the Colebrook-White Correlation[5] is used in RELAP5-3D.

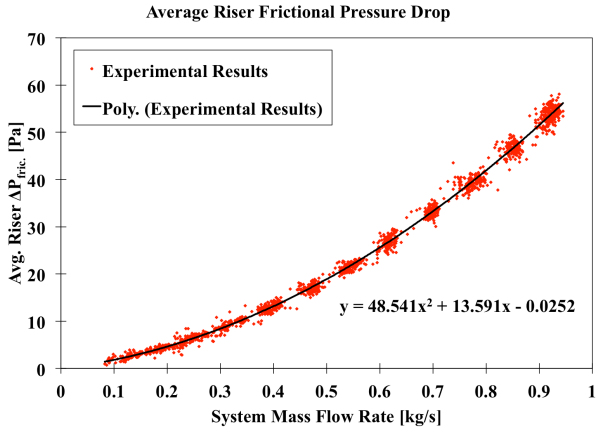

Fig. 5. Average experimental riser frictional pressure drop results.

TABLE II. Model Verification for Riser Frictional Pressure Drop

Parameters	Values
Mass Flow Rate	0.548 kg/s
Calculated from Experimental Data Δp*	22.00 Pa
RELAP5 Δp*	21.85
Percent Error	0.68%

* This is the pressure difference due to friction only

II.B. Base Case Simulation Results

Following modifications to the RELAP5-3D model of the NSTF, full test simulations were performed to confirm experimental data. The experimental data was collected during Run011, a baseline run conducted on 1/28/15. For this experiment, the facility was placed in a natural circulation configuration, meaning that the valves were positioned to direct flow through the north and south chimneys instead of through the ductwork associated with a forced flow test that contain fans. As the test began, the electrical power (used to heat the reactor vessel analogue) was increased from 0 kW to 56.07 kW over a 2 hour period. The power level remained at 56.07 kW for 19 hours and 14 minutes, before increasing to 82.00 kW over another 2 hour period. The power level remained at 82.00 kW for 22 hours and 22 minutes at which point it was reduced to zero over a 3 hour and 57 minute period. The complete power profile is shown in Fig. 6.

Fig 6 also includes the power introduced into the RELAP5-3D simulation in the riser ducts. Due to losses in the system, there is a significant difference in the magnitudes of these two curves. The simulation input power was calculated from experimental data collected using thermocouples located at the inlet of each riser duct and Luna fibers located at the outlet of each riser duct. Because the walls of the riser ducts are heated, a temperature profile in the air passing through the riser ducts exists with higher temperatures near the heated

surfaces and lower temperatures in the center of the riser ducts. Therefore, a single point measurement at the outlet of a riser duct would not provide an accurate air temperature, whereas a Luna fiber does. The model input power curve shown in Fig. 6 was estimated by averaging the Luna fiber data[6] for each duct and then taking the average outlet air temperature of all twelve riser ducts.

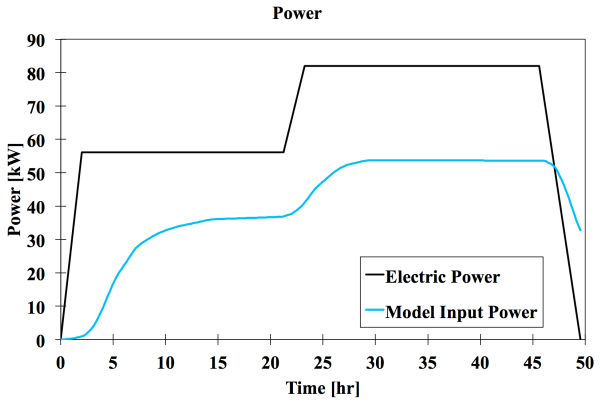

Fig. 6. Electrical and model input power profiles.

The results from both the experimental data from Run011 and the RELAP5-3D model are provided in the remainder of this section. The results of the mass flow rate of air in the downcomer are shown in Fig. 7. In general, the mass flow rate of the model closely matches that of the experiment. The difference between the two is attributed to two sources. The first is that in the RELAP5-3D model, the air pressures interior and exterior to the building are equal. In reality, this is not true as the presence of the building itself and the operation of the building's HVAC system will induce a pressure difference. The second explanation for the difference in mass flow rates is more heat is lost in the chimneys of NSTF than in the simulation. Heat losses in the chimneys increase the density of the air flowing through them, which reduces the driving head of the facility. The NSTF staff is currently investigating the effects of the pressure difference inside and outside the building and the heat losses in the upper chimneys.

The results of the riser differential pressure drop are shown in Fig. 8. The experimental results were determined by averaging the pressure drop over all twelve riser ducts. The pressure difference across the riser ducts has three components: the hydrostatic head, the frictional pressure drop, and a pressure drop due to the acceleration of air in the heated riser ducts. The results from the model closely match those of the experimental data.

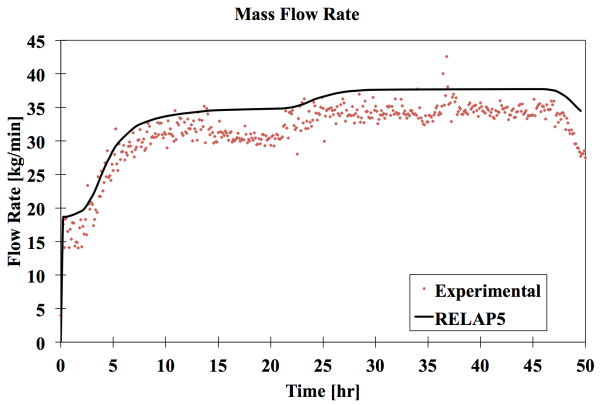

Fig. 7. Mass flow rate results comparison.

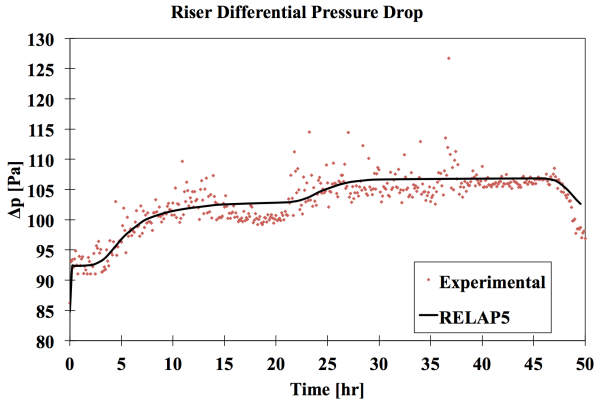

Fig. 8. Riser differential pressure drop results comparison.

The average temperature rise of the air passing though the hot riser ducts is shown in Fig. 9. The differences observed between the experimental data and the model results are due to the difference in mass flow rate shown in Fig. 7.

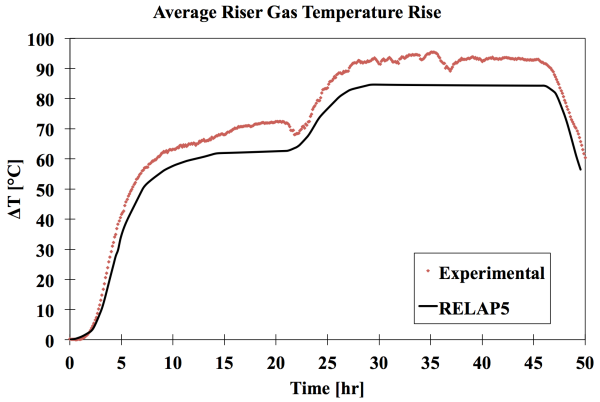

Fig. 9. Average riser air temperature rise results comparison.

The temperature results of the air in the outlet plenum and in the chimney ducts are shown in Fig. 10 and Fig. 11 respectively. In both figures, the RELAP5 results over-predict the temperature data from Run011 even though the average air temperature rise in the risers was higher in the experimental data than in the simulation results. The experimental data for the outlet plenum air temperature is averaged from measurements recorded by a thermocouple assembly located along the centerline of the outlet plenum. Following Run011, it was discovered that small gaps existed at the joints of the outlet plenum insulation panels, and minor air leakages were occurring. These air leakages have since been addressed in the test facility, but minor discrepancies were created in the post-analysis comparisons between the experimental data of the specific test and simulation results in the outlet plenum.

The air temperature drops from the elbows to the stacks of the chimneys are significantly higher in the experimental results than in the RELAP5-3D simulation results (approximately 12°C compared to 3°C). Further investigations are being conducted to better understand the heat losses and/or identify issues associated with insulation along the chimney region of the facility.

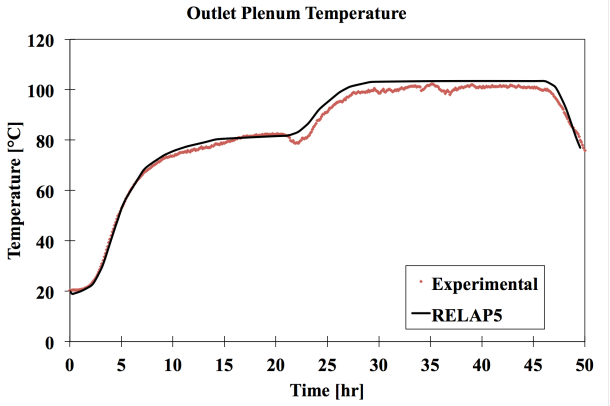

Fig. 10. Outlet plenum air temperature results comparison.

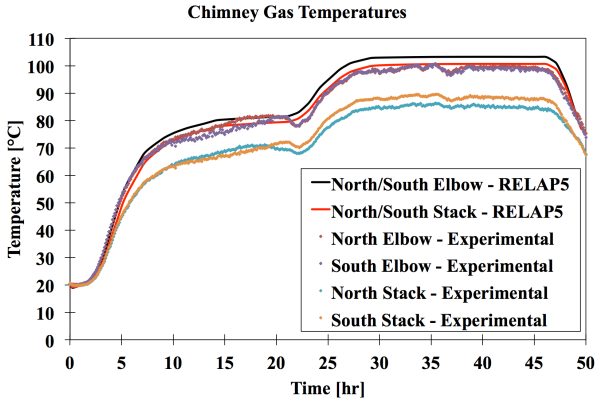

Fig. 11. Chimney air temperature results comparison.

Velocity measurements taken with pitot tubes located in the chimney ductwork of the NSTF were similar to the velocities predicted by the RELAP5-3D simulation. The results are shown in Fig. 12. The experimental results did exhibit significant deviation even during the steady-state periods, but the RELAP5-3D model results fell within the envelope of those deviations.

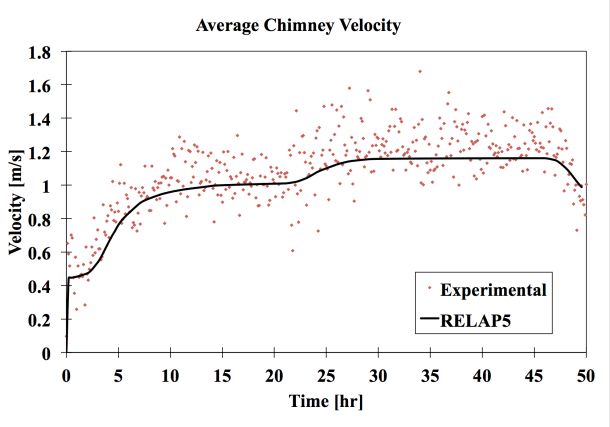

Fig. 12. Average chimney air velocity results comparison.

II.C. Effects of Ambient Air Temperature

The effects of the temperature of the atmosphere, both inside and outside Building 308 at Argonne, were investigated with the RELAP5-3D model of the NSTF. The goal of this study was to determine how the facility would function at extreme air inlet and outlet temperatures. The main goal of varying the inlet air temperature was to determine how the facility would perform if Run011 had been conducted during the summer months instead of the winter (the HVAC system of Building 308 does not have cooling capabilities). The effects of the outside air temperature were investigated to characterize the losses of the upper chimneys that are located above the roofline of Building 308. Details of the indoor and outdoor air temperatures for each simulation performed during this study are provided in Table III. The input power of each scenario was identical to the power profile shown in Fig. 6 for Run011.

TABLE III. Indoor/Outdoor Air Temperatures of Simulations.

Simulation#	Indoor Air Temperature [°C]	Outdoor Air Temperature [°C]
1	20	1
2	20	-40
3	20	40
4	40	40

Simulations 1 through 3 produced nearly identical results because the temperatures of air being drawn into

the system in all three simulations were the same. In RELAP5-3D, a time-dependent volume at the inlet of a system is used to set the temperature boundary condition of that system, while a time-dependent volume at the outlet of the system determines the pressure boundary condition of that system. The results from simulation 4 differed significantly from the others because its inlet temperature was 20°C higher than the other 3 simulations. The results of the mass flow rate, average riser differential pressure drop, and average riser gas temperature rise for simulation 1 and 4 are provided in Fig. 13 through Fig. 15.

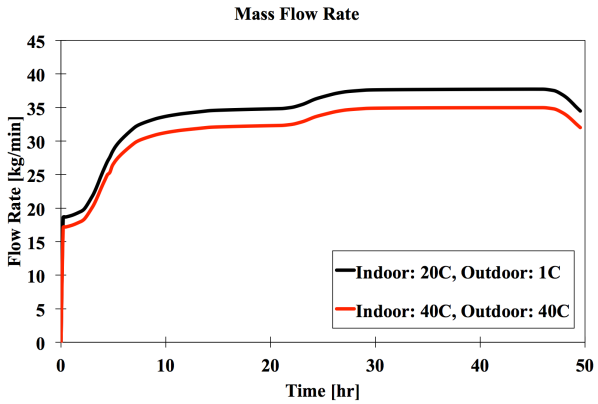

Fig. 13. Simulation mass flow rate comparison.

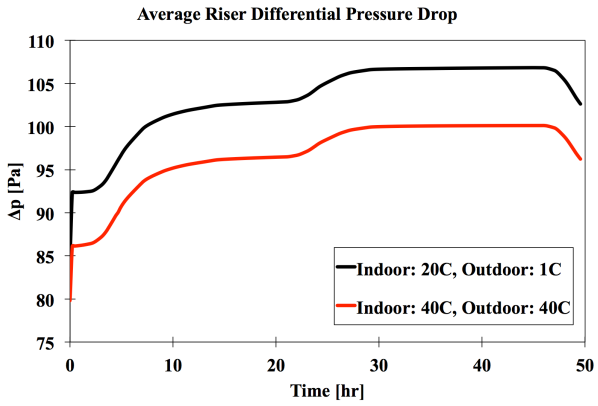

Fig. 14. Simulation average differential pressure drop across riser ducts comparison.

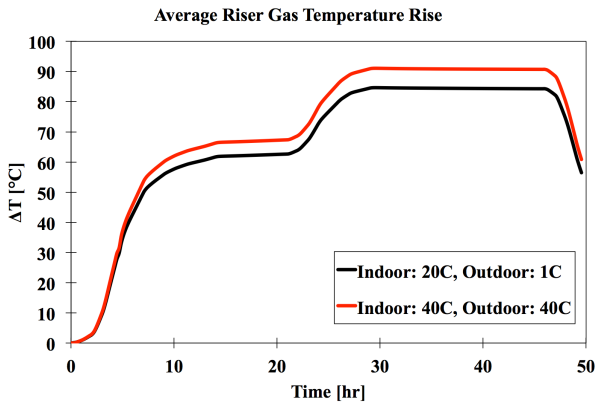

Fig. 15. Simulation average riser air temperature rise comparison.

The mass flow rate was lower for simulation 4 compared to simulation 1. This is due to the relationship between air density and temperature. Air density does not decrease linearly with increasing temperature. As air temperature increases, the rate of change of the air density with respect to temperature decreases. Therefore, at steady-state flow conditions, higher inlet temperatures will lead to lower density differences between the air in the cold downcomer and the air in the hot riser ducts and chimneys. This lower density difference in simulation 4 results in a lower mass flow rate through the system and an increased air temperature rise over the riser ducts even though the input power for both simulations was identical.

It should be noted that the outer surface of the upper half of the ductwork of the two chimneys is exposed to the environment outside Building 308. In theory, this should lead to different results for simulation 1 through 3. Since the outside air temperature of simulation 2 is 41°C lower than that of simulation 1, it would be expected that simulation 2 would experience significantly more heat loss through the chimney duct walls than simulation 1. Similarly, it would be expected that simulation 3 would experience less heat loss through the chimney duct walls because the outside air temperature is 39°C higher than that of simulation 1. However, the ductwork of the chimneys is insulated and that insulation material is included in the RELAP5-3D model of the NSTF. To highlight the effects of the insulation on the system performance, Table IV provides maximum temperature values of the chimney air, duct wall, and outer insulation for all three scenarios. The results demonstrate that even though the outdoor air temperature affects the outer insulation temperature and duct wall temperature, the overall effect on the chimney air temperature (and therefore the effect on the performance of the system) is minimal. It should be noted that the air temperature drop across the chimney stacks was much higher in the experimental results (see Fig. 11). Further investigations

are being conducted to better understand the heat losses in the chimney region of the facility.

TABLE IV. Simulation Maximum Temperatures in the Chimney Region.

Parameter	Outdoor Air Temperature		
	40°C	1°C	-40°C
Chimney Air Temp.	99.7	99.6	99.5
Duct Wall Temp.	93.1	88.4	83.2
Outer Insulation Temp.	63.2	35.7	5.1

III. CONCLUSIONS

A RELAP5-3D model of the NSTF was developed and utilized to perform transient analyses. Some model verification and validation work was performed on the main components of the model. Simulation results were compared to experimental results from Run011 conducted at the NSTF. Overall, the simulation results compared favorably to the experimental data, however, further analyses will need to be conducted to investigate identified differences. Also, facility modifications have been or are being performed to address differences in simulation results and experimental data.

The effects of the air temperature inside and outside the facility were investigated using the RELAP5-3D model of the NSTF. The results indicate that the performance of the system differs for different building interior air temperatures, but if the chimney duct walls are well insulated, the building exterior air temperature has little effect on the system performance. It is important to note that in the full-scale RCCS, the air inlet is located exterior to the reactor building, whereas the NSTF air inlet is located inside of Building 308 at Argonne. Therefore, it would be expected that the functionality of the full-scale RCCS would differ at different building exterior air temperatures.

ACKNOWLEDGMENTS

Argonne National Laboratory's work was supported by the U.S. Department of Energy, Assistant Secretary for Nuclear Energy, Office of Nuclear Energy, under contract DE-AC02-06CH11357.

REFERENCES

1. "Preliminary Safety Information Document for the Standard MHTGR," HTGR-86-024, Vol. 1, Amendment 13, U.S. Department of Energy (1992).
2. S. Lomperski, W. D. Pointer, C. P. Tzanos, et al., "RCCS Studies and NSTF Preparation Air-Cooled Option," ANL-GenIV-142, Argonne National Laboratory (2010).
3. S. Lomperski, W. D. Pointer, C. P. Tzanos, et al., "Generation IV Nuclear Energy System Initiative: Air-Cooled Option RCCS Studies and NSTF Preparation", ANL-GenIV-179, Argonne National Laboratory (2011).
4. D. Lisowski, M. Farmer, et al., "Design Report for the 1/2 Scale Air-Cooled RCCS Tests in the Natural convection Shutdown Heat Removal Test Facility (NSTF)", ANL-SMR-8, Argonne National Laboratory (2014).
5. The RELAP5-3D Code Development Team, "RELAP5-3D Code Manual," INEEL-EXT-98-00834, Rev. 4, Idaho National Laboratory (2012).
6. D. Lisowski, A. Kraus, M. Bucknor, and R. Hu, "Separate Effects Characterization of the NSTF to Support Computational Modeling", Proc. of ANS Winter 2015, Washington, DC, Nov. 8-12, (2015).